

Modifying surgical implantation of deep brain stimulation leads significantly reduces RF-induced heating during 3 T MRI

Jasmine Vu, Bhumi Bhusal, Joshua Rosenow, Julie Pilitsis, and Laleh Golestanirad, *Member, IEEE*

Abstract—Radiofrequency (RF) heating of tissue during magnetic resonance imaging (MRI) is a known safety risk in the presence of active implantable medical devices (AIMDs). As a result, access to MRI is limited for patients with these implants including those with deep brain stimulation (DBS) systems. Numerous factors contribute to excessive RF tissue heating at the DBS lead-tip, most notable being the trajectory of the lead. Phantom studies have demonstrated that looping the extracranial portion of the DBS lead at the surgical burr hole reduces the heating at the lead-tip; however, clinical implementation of this technique is challenging due to surgical constraints. As such, the intended looped trajectory is usually different from what is implanted in patients. To date, no data is available to quantify the extent by which surgical trajectory modification reduces RF heating of DBS leads compared to the typical surgical approach. In this work, we measured RF heating of a commercial DBS system during 3 T MRI, where the trajectory of the lead and extension cable mimicked lead trajectories constructed from postoperative CT images of 13 patients undergoing modified DBS surgery and 2 patients with unmodified trajectories. Two manually created trajectories mimicking typical heating cases seen in the literature were also evaluated. We found that modified lead trajectories reduced the average heating by 3-folds compared to unmodified lead trajectories.

Clinical Relevance— This study evaluates the performance of a surgical modification in the routing of DBS leads in reducing RF-induced heating during MRI at 3 T.

I. INTRODUCTION

Magnetic resonance imaging (MRI) is a widely used neuroimaging modality that offers high resolution and excellent soft tissue contrast through a noninvasive procedure. The need for MRI exams continues to burgeon, particularly for patients with active implantable medical devices (AIMDs). Notably, approximately 70% of patients with deep brain stimulation (DBS) implants will require an MRI exam within 10 years following device implantation [1]. Despite recent advances in implant and MRI technology, MRI-induced radiofrequency (RF) tissue heating remains a major safety concern for patients with DBS systems. Localized excessive heating accumulates at the interface of

the lead-tip and tissue since the lead behaves like an antenna when coupled with the electric field of the MRI transmit coil. This interaction amplifies the specific absorption rate (SAR) of RF energy in the surrounding tissue [2], [3]. Due to the risk of RF heating, MRI protocols for patients with implanted DBS systems are highly restricted. To date, head imaging is limited to a magnetic field strength of 1.5 T with a heating-related threshold of a $B_{1+rms} < 1.1 \mu T$ based on established guidelines for Abbott Medical MR-conditional full DBS systems [4]. These stringent guidelines limit MRI protocols for evaluating potential post-surgical complications and optimal structural imaging using 3 T MRI.

RF-induced tissue heating is a multiparameter phenomenon; the orientation and trajectory of an implanted lead are key contributors to significant variations in RF tissue heating [5]–[9]. Recently developed approaches for mitigating RF-induced heating for DBS patients include modifying the material and design of DBS leads, introducing novel MRI coil technology to induce a region of low electric field that coincides with the implanted lead's trajectory, and performing exams at a vertical scanner with a different orientation of the magnetic and electric fields [10]–[17]. However, these methods require modifications to existing DBS or MRI technology. On the contrary, surgically placing the extracranial portion of the DBS lead into concentric loops near the respective burr-hole reduces RF tissue heating by minimizing the exposure to the maximum tangential electric field without altering the DBS system [7]. This surgical lead management approach with modified lead trajectories has been demonstrated in simulation-based and experimental studies with isolated DBS leads or with limited cohorts [7], [18].

It is important to note, however, that in contrast to phantom studies that allow for easy manipulation and positioning of the leads, trajectory modification in a clinical setting is far more challenging due to surgical constraints. In DBS surgery, a linear incision is made in the scalp through which the extracranial portion of the lead is tucked under the skin. As such, surgeons cannot visually inspect the lead trajectory, and for this reason the intended trajectory (i.e., having concentric loops at the burr hole) is usually different from what is

*Research supported by National Institute of Health grants R00EB021320.
Corresponding author: L. Golestanirad

J. Vu and L. Golestanirad are with the Department of Biomedical Engineering, McCormick School of Engineering, Northwestern University, Evanston, IL, USA and the Department of Radiology, Feinberg School of Medicine, Northwestern University, Chicago, IL, USA (e-mail: laleh.rad1@northwestern.edu).

B. Bhusal is with the Department of Radiology, Feinberg School of Medicine, Northwestern University, Chicago, IL, USA.

J. Rosenow is with the Department of Neurosurgery, Feinberg School of Medicine, Northwestern University, Chicago, IL, USA.

J. Pilitsis is with the Department of Neurosciences & Experimental Therapeutics, Albany Medical College, Albany, NY, USA.

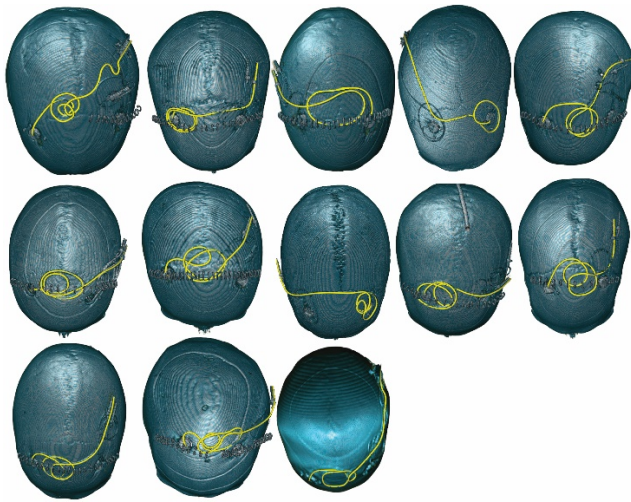


Figure 1. 3D surface rendered views of CT images of patients with implanted modified DBS lead trajectories. DBS lead trajectories that were evaluated in this study are highlighted (yellow).

implanted in patients. To date, no data is available to quantify the effect of clinical trajectory modification compared to the typical surgical approach.

In this study, we evaluated the effect of surgical modification of extracranial DBS lead trajectories on reducing RF-induced tissue heating. We performed RF heating experiments at 3 T MRI with a commercial DBS system implanted in a realistic anthropomorphic phantom. We measured the maximum temperature rise, ΔT , for 15 patient-derived DBS lead trajectories reconstructed from postoperative CT images of patients undergoing DBS surgery at our institutions, as well as 2 additional lead trajectories that mimicked typical routing of DBS leads as seen in other publications. Results from these experiments demonstrate that clinical implementation of trajectory modification is highly effective in reducing RF heating during 3 T MRI.

II. METHODS

A. Patient-derived DBS Lead Trajectories

In total, 17 unique, clinically relevant DBS trajectories were evaluated in this study. DBS lead trajectories were reconstructed from postoperative computed tomography (CT) images of patients who underwent DBS surgery at Albany Medical Center (AMC) performed by a single neurosurgeon. These trajectories varied in both loop size and location on the skull across these patients (Fig. 1). Use of patients' imaging data for modeling purposes was approved by AMC's Institutional Review Boards. Modified DBS lead trajectories were classified as trajectories with loops near the surgical burr-hole, reflecting an approach found to minimize RF-induced tissue heating [7], [19]. Each DBS lead was identified in the patient CT images using 3D Slicer 4.10.2 (<http://slicer.org>). The corresponding coordinates of points along the trajectory of each lead were extracted and processed in a CAD tool (Rhino 6.0, Robert McNeal & Associates, Seattle, WA) to create a 3D model of each DBS lead trajectory. These models were 3D-printed in ABS plastic and served as guides for the RF heating experiments. 3D-printed guides were then used to shape a commercial DBS lead along

different trajectories to assure that the orientation and positioning of the lead were realistically replicated (Fig. 2). Note that the guide was detached from the lead after the trajectory was fixed on to the skull phantom with tape.

B. RF Heating Experiments

An anthropomorphic phantom of the human head and torso and a skull was constructed for RF heating experiments similar to our previous work [20]. Briefly, the phantom was derived from postoperative CT images of a patient, with the head, torso, and skull segmented using 3D Slicer 4.10.2 (Fig. 2). Further processing was completed in Rhino 6.0 to create triangulated surfaces for 3D printing. The skull consisted of corresponding halves divided along the coronal plane to allow for positioning of the intracranial portion of the lead. All components of the phantom were 3D-printed in ABS plastic and coated with acrylic for waterproofing. Tissue-mimicking gel was created from a solution of agar (32 g/L) (Landor Trading Co., gel strength of 900 mg/cm²), NaCl (2.25 g/L), and water. The electric conductivity and relative permittivity of the agar-based gel were 0.40 S/m and 77, respectively, as measured using a vector network analyzer (Keysight Technologies, Santa Rosa, CA). The skull was filled with this agar-based gel which prevented convection during RF heating measurements while the head-torso part of the phantom was filled with 18 L of saline solution ($\sigma = 0.50$ S/m, $\epsilon_r = 80$) to allow for complete submersion of the lead, extension, and implantable pulse generator (IPG) in the saline solution.

Heating experiments were performed with a full commercial DBS system from Abbott (St. Jude Medical, Plano, TX) including a 40 cm 8-channel directional lead (model 6173), a 50 cm extension (model 6371), and an IPG (Infinity 6660). Fluoroptic temperature probes (OSENSA, BC, Canada) were used to measure ΔT at the tip of the DBS lead. Temperature probes were securely attached to the DBS lead at the distal end at electrodes 1 and 2. The DBS lead and

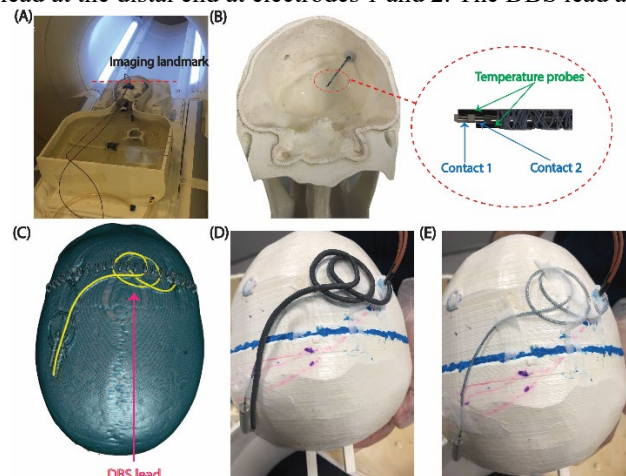


Figure 2. Experimental setup. (A) Anthropomorphic phantom with the full DBS system implanted. (B) Cross-sectional view of the skull phantom with the inserted DBS lead and securely attached temperature probes. (C) 3D surface rendered view of a CT image of a patient with implanted DBS leads. An example of an evaluated lead trajectory is highlighted (yellow). (D) A 3D-printed model of the respective DBS lead trajectory (black) was used as a guide to replicate the trajectory for RF heating experiments. (E) The trajectory of the commercial DBS lead was shaped to match the patient-derived trajectory as indicated in the CT image.

temperature probes were inserted into the skull through a 5 mm hole; placement of the lead and probes mimicked the location and angle of insertion for targeting the subthalamic nucleus (STN). The extracranial region of the DBS lead was routed along different patient-derived trajectories using the 3D-printed guides to evaluate the effect of the trajectory on the temperature rise at the DBS lead-tip. The lead was connected to the extension and IPG; the extension was routed laterally along the neck with looping around the IPG to account for any excess length while the IPG was placed in the pectoral region contralateral to the implanted lead.

Prior to and following RF heating experiments, we used the Clinician Programmer Application to measure the impedances on the electrode array to verify the DBS system's integrity and to assess for any interference with the DBS system's function due to the RF exposure. No problems were detected during the impedance measurements.

Heating experiments were performed at a Siemens 3 T Prisma scanner (Siemens Healthineers, Erlangen, Germany) with a body transmit coil and a 20-channel receive head coil. The phantom was placed in the head-first, supine position, and the imaging landmark for all experiments was located at the level of the DBS lead-tip, corresponding to neuroimaging for DBS patients. RF exposure for these experiments at 3 T was generated using a high-SAR T1-weighted turbo spin echo (TSE) sequence (TE = 7.5 ms, TR = 1450 ms, FA = 150°, FOV = 180 mm x 180 mm, number of slices = 70, acquisition time = 451 seconds, voxel size = 0.9 mm x 0.9 mm x 1.4 mm, B_1^{+rms} = 2.8 μ T). The temperature was measured throughout the duration of RF exposure. Ample time was allotted to allow for the temperature to return to the baseline temperature following each experiment. Each experimental configuration included only one DBS lead with one lead trajectory to represent scenarios with unilateral DBS.

III. RESULTS

A total of 17 trajectories were assessed, including 13 patient-derived modified trajectories, 2 patient-derived unmodified trajectories, and 2 manually created trajectories mimicking typical cases seen in the literature. In all evaluated configurations, the implanted lead was contralateral to the IPG. The extracranial trajectories that demonstrated typical RF heating scenarios typically included an uncoiled region around the burr-hole or with loops on the border of temporal and occipital bones. Modified extracranial trajectories contained loops near the respective surgical burr-hole.

The measured ΔT occurred in the agar-based gel immediately surrounding the DBS lead-tip during all experiments. DBS leads with modified trajectories had a ΔT of 0.18-1.49 °C with mean \pm standard deviation of 0.75 ± 0.33 °C. On the contrary, the DBS leads with the unmodified trajectories showed a substantially greater ΔT than the modified lead trajectories with $\Delta T = 2.18 \pm 0.06$ °C. Most notably, the DBS lead trajectories with a straight segment passing the skull mediolaterally and a loop positioned at the border of the temporal and occipital bones demonstrated a ΔT of 7.75 °C and 11.97 °C.

Figure 3 shows the distribution of the maximum temperature rise for the modified lead trajectories fitted to a

Rayleigh distribution ($\sigma = 0.38$) using the Distribution Fitter App of Matlab 2018b. The confidence interval of ΔT with a 95% confidence level is 0.57-0.98 °C. RF heating for the unmodified lead trajectories with the typical heating configurations far exceeds two standard deviations of the average ΔT measured for the modified DBS lead trajectories.

IV. DISCUSSION AND CONCLUSIONS

Currently, DBS is the gold-standard for addressing movement disorders, and the clinical use of DBS for treating other neurological and psychiatric disorders is under ongoing evaluations [21]. Similarly, the need for MRI for DBS patients continues to increase as MRI allows for superior target verification while fMRI provides greater understanding of the mechanisms of DBS [22]–[24].

The problem of RF heating in the tissue around DBS leads remains a significant barrier to 3 T MRI for DBS patients. Surgical lead management is one effective method with demonstrated surgical feasibility for mitigating RF heating without altering surgical planning and implantation procedures of the intracranial region of the lead [7], [19]. Previous works show that manipulating the extracranial trajectory of DBS leads into loops around the burr-hole consistently reduces RF heating. In this work, we studied the effect of modified extracranial DBS lead trajectories that were implanted in patients on RF heating. All RF heating experiments were performed with a commercial full DBS system at a 3 T MRI scanner. We observed substantially reduced heating around the DBS lead-tip for modified trajectories compared to trajectories that displayed typical heating scenarios. Additionally, all leads with modified trajectories had a ΔT below 2 °C. One mechanism for the lower measured ΔT due to the presence of the extracranial loops around the burr-hole includes cancellation of the tangential component of the incident electric field along the initial segment of the lead that exits the burr-hole [7].

While implementing the extracranial loops in the DBS lead trajectory reduced RF heating, several limitations remain. The amount of heating measured is specific to the model of the DBS system, the MRI scanner, and the patient-derived lead trajectories used in this study and cannot be extrapolated to DBS systems from other commercial vendors. Additionally, experiments were performed with a unilateral lead in a single phantom setup; it has been highlighted that different patient body compositions affect RF heating due to differences in electric properties around the implanted DBS system [20]. Future work will include a systematic assessment of RF heating accounting for these related factors.

ACKNOWLEDGMENT

This work was supported by National Institute of Health grant R00EB021320.

REFERENCES

- [1] S. Falowski, Y. Safriel, M. P. Ryan, and L. Hargens, "The Rate of Magnetic Resonance Imaging in Patients with Deep Brain Stimulation," *Stereotact. Funct. Neurosurg.*, vol. 94, no. 3, pp.

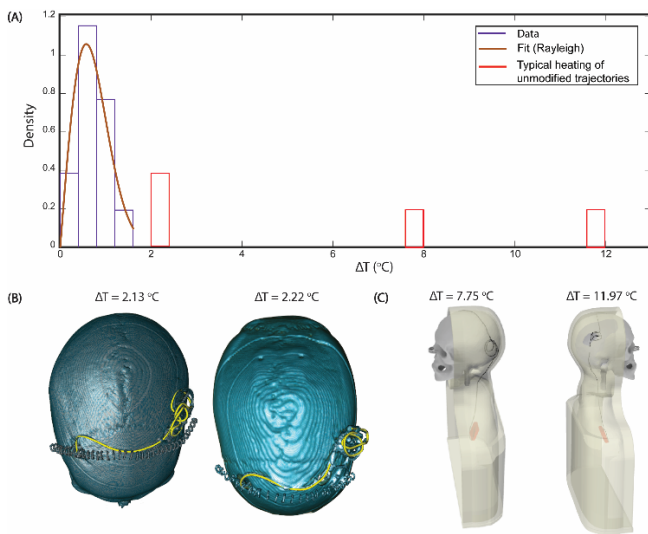


Figure 3. (A) Distribution of ΔT for the 13 modified DBS lead trajectories. The distribution was fitted to the Rayleigh distribution. The distribution of ΔT for the lead trajectories representing typical heating scenarios is also included. (B) 3D surface rendered view of patient CT images with examples of DBS lead trajectories with typical heating scenarios. The measured ΔT values from the RF heating experiments are indicated for the highlighted DBS lead trajectories and are outside the 95% confidence interval estimated under the Rayleigh distribution of ΔT for DBS leads with modified trajectories. (C) 3D rendered view of manually created DBS lead trajectories that were evaluated.

147–153, Aug. 2016.

[2] A. R. Rezai *et al.*, “Neurostimulation systems for deep brain stimulation: In vitro evaluation of magnetic resonance imaging-related heating at 1.5 Tesla,” *J. Magn. Reson. Imaging*, vol. 15, no. 3, pp. 241–250, Mar. 2002.

[3] A. R. Rezai *et al.*, “Neurostimulation System Used for Deep Brain Stimulation (DBS): MR Safety Issues and Implications of Failing to Follow Safety Recommendations,” *Invest. Radiol.*, vol. 39, no. 5, pp. 300–303, 2004.

[4] S. J. Medical, “MRI procedure information for St. Jude Medical MR conditional deep brain stimulation system,” 2018.

[5] E. Mattei *et al.*, “Complexity of MRI induced heating on metallic leads: Experimental measurements of 374 configurations,” *Biomed. Eng. Online*, vol. 7, no. 1, p. 11, Mar. 2008.

[6] L. Golestanirad, L. M. Angelone, M. I. Iacono, H. Katnani, L. L. Wald, and G. Bonmassar, “Local SAR near deep brain stimulation (DBS) electrodes at 64 and 127 MHz: A simulation study of the effect of extracranial loops,” *Magn. Reson. Med.*, vol. 78, no. 4, pp. 1558–1565, 2017.

[7] L. Golestanirad *et al.*, “RF-induced heating in tissue near bilateral DBS implants during MRI at 1.5 T and 3T: The role of surgical lead management,” *Neuroimage*, vol. 184, pp. 566–576, Jan. 2019.

[8] J. Vu, B. Bhusal, B. T. Nguyen, and L. Golestanirad, “Evaluating Accuracy of Numerical Simulations in Predicting Heating of Wire Implants During MRI at 1.5 T,” in *42nd Annual International Conference of the IEEE Engineering in Medicine & Biology Society (EMBC)*, 2020, pp. 6107–6110.

[9] L. Golestanirad *et al.*, “Changes in the specific absorption rate (SAR) of radiofrequency energy in patients with retained cardiac leads during MRI at 1.5T and 3T,” *Magn. Reson. Med.*, vol. 81, no. 1, pp. 653–669, 2019.

[10] P. Serano, L. M. Angelone, H. Katnani, E. Eskandar, and G. Bonmassar, “A novel brain stimulation technology provides compatibility with MRI,” *Sci. Rep.*, vol. 5, no. 1, p. 9805, Sep. 2015.

[11] L. Golestanirad *et al.*, “Reducing RF-Induced Heating Near Implanted Leads Through High-Dielectric Capacitive Bleeding of

Current (CBLOC),” *IEEE Trans. Microw. Theory Tech.*, vol. 67, no. 3, pp. 1265–1273, Mar. 2019.

[12] L. Golestanirad *et al.*, “Construction and modeling of a reconfigurable MRI coil for lowering SAR in patients with deep brain stimulation implants,” *Neuroimage*, vol. 147, pp. 577–588, 2017.

[13] E. Kazemivalipour *et al.*, “Reconfigurable MRI technology for low-SAR imaging of deep brain stimulation at 3T: Application in bilateral leads, fully-implanted systems, and surgically modified lead trajectories,” *Neuroimage*, vol. 199, pp. 18–29, 2019.

[14] L. Golestanirad *et al.*, “Reconfigurable MRI coil technology can substantially reduce RF heating of deep brain stimulation implants: First in-vitro study of RF heating reduction in bilateral DBS leads at 1.5 T,” *PLoS One*, vol. 14, no. 8, 2019.

[15] L. Golestanirad *et al.*, “RF heating of deep brain stimulation implants in open-bore vertical MRI systems: A simulation study with realistic device configurations,” *Magn. Reson. Med.*, vol. 83, no. 6, pp. 2284–2292, 2019.

[16] C. E. McElcheran, B. Yang, K. J. T. Anderson, L. Golestanirad, and S. J. Graham, “Parallel radiofrequency transmission at 3 tesla to improve safety in bilateral implanted wires in a heterogeneous model,” *Magn. Reson. Med.*, vol. 78, no. 6, pp. 2406–2415, Dec. 2017.

[17] C. E. McElcheran *et al.*, “Numerical Simulations of Realistic Lead Trajectories and an Experimental Verification Support the Efficacy of Parallel Radiofrequency Transmission to Reduce Heating of Deep Brain Stimulation Implants during MRI,” *Sci. Rep.*, vol. 9, p. 2124, 2019.

[18] B. Davidson *et al.*, “Three-Tesla Magnetic Resonance Imaging of Patients With Deep Brain Stimulators: Results From a Phantom Study and a Pilot Study in Patients,” *Neurosurgery*, vol. 0, no. 0, pp. 1–7, 2020.

[19] K. B. Baker, J. Tkach, J. D. Hall, J. A. Nyenhuis, F. G. Shellock, and A. R. Rezai, “Reduction of magnetic resonance imaging-related heating in deep brain stimulation leads using a lead management device,” *Oper. Neurosurg.*, vol. 57, no. 4 SUPPL., 2005.

[20] B. Bhusal *et al.*, “Effect of Device Configuration and Patient’s Body Composition on the RF Heating and Nonsusceptibility Artifact of Deep Brain Stimulation Implants During MRI at 1.5T and 3T,” *J. Magn. Reson. Imaging*, Aug. 2020.

[21] A. M. Lozano *et al.*, “Deep brain stimulation: current challenges and future directions,” *Nat. Rev. Neurol.*, vol. 15, no. 3, pp. 148–160, 2019.

[22] I. Hancu *et al.*, “On the (Non-)equivalency of monopolar and bipolar settings for deep brain stimulation fMRI studies of Parkinson’s disease patients,” *J. Magn. Reson. Imaging*, vol. 49, no. 6, pp. 1736–1749, Jun. 2019.

[23] M. Dimarzio *et al.*, “Functional MRI Signature of Chronic Pain Relief from Deep Brain Stimulation in Parkinson Disease Patients,” *Clin. Neurosurg.*, vol. 85, no. 6, pp. E1043–E1049, Dec. 2019.

[24] M. DiMarzio *et al.*, “Use of Functional MRI to Assess Effects of Deep Brain Stimulation Frequency Changes on Brain Activation in Parkinson Disease,” *Neurosurgery*, vol. 88, no. 2, pp. 356–365, 2020.